Interferometric Methods for Suppressing Additive Noise

V. M. Nikitin[1*], V. A. Sautkin[2], V. N. Fomin[3***], and A. B. Tserevitinov[3****]**

[1] *National Research University "Belgorod State University", ul. Pobedy 85, Belgorod, 308015 Russia*
[2] *JSC "Krasnogorsky Zavod", ul. Rechnaya 8, Krasnogorsk, Moscow Oblast, 143403 Russia*
[3] *Prokhorov General Physics Institute, Russian Academy of Sciences, ul. Vavilova 38, Moscow, 119991 Russia*

Abstract—Interferometric methods for signal processing, which make it possible to obtain a better noise protection of information laser and optoelectronic systems during detection and processing of optical fields under conditions for external additive noise, are proposed based on the results of analysis of the specific features of field formation in passive and active optical interferometers. The possibility of reducing the effect of external factors on the efficiency of additive-noise suppression by supplementing an interferometer with a stimulated-Brillouin-scattering fiber mirror is investigated. The technical feasibility of the methods proposed is shown and their efficiency is experimentally confirmed.

DOI: 10.3103/S1541308X14020058

1. INTRODUCTION

The rapid progress of laser and optoelectronic technologies in all fields of fundamental and applied research gave a new impetus to the development of optical interferometry and made it possible to expand significantly its application range. Currently, interferometric methods are an actively developing line of research in physical and applied optics, which uses the latest achievements of laser technique, optoelectronics, and fiber optics and is applied in various fields. Currently, double-beam interferometers (such as Mach–Zehnder interferometer and its various modifications) are widely used in designing highly sensitive precise optical sensors and gyroscopes and in other important fields of science and technology, including astrophysical systems for observing distant objects and systems for diagnostics of various physical processes (see, for example, [1–8]). The constant interest in the transformation of optical fields by interferometric methods is related to the possibility of implementing direct optical processing of optical fields and controlling their spatial and temporal structure. At the same time, an analysis of the modern state of the problems related to the development and application of interferometric methods shows that their unique potential for various applied problems has not been realized and implemented in full measure. Thus, there is a wide area of activity for researchers and experts in this field. Here, we consider one of applications of interferometric methods aimed at improving the noise protection of laser and optoelectronic information systems applied in detection and processing of optical fields under conditions of external additive noise.

*E-mail: nikitin@bsu.edu.ru
**E-mail: sautkin@zenit-kmz.ru
***E-mail: vnfomin@yandex.ru
****E-mail: A.Tserevitinov@yandex.ru

2. SPATIAL AND TEMPORAL SELECTION OF NOISE IN A PASSIVE INTERFEROMETER

2.1. Formation of Fields in a Passive Interferometer

Let us consider some specific features of field formation at outputs of a passive optical interferometer. Generally, interferometer arms are characterized by some relative temporal and spatial mismatch, which is caused by various factors. The spatial wave mismatch (Δx) in the interferometer arms characterizes their angular mismatch, while the temporal mismatch Δt is characteristic of the optical lengths of different interferometer arms. We assume that a plane coherent monochromatic wave E (an additive mixture of signal and noise) arrives at the interferometer input. In this case, the amplitude $|E|$ is related to the arrival rate of signal and noise photons. Note that the results obtained in this study for monochromatic waves can be expanded to optical fields of complex spectral composition [9] and that the term "coherent" does not necessarily imply limited consideration of only laser sources, because partially coherent light can be formed by sources of other types, emitting in a wide spectral range.

The complex wave amplitudes in the first and second interferometer arms can be found from the relation [10]

$$|E_1| = |E_2| = |E|/\sqrt{2}. \tag{1}$$

Mixing of waves with the amplitudes

$$|E_{11}| = |E_{12}| = |E_{21}| = |E_{22}| = E/\sqrt{2} \tag{2}$$

occurs at the interferometer outputs.

The total light intensity at the first output of the interferometer is found from the relation

$$\begin{aligned} I_{P_1} &= \Big\langle \big[E_{11}(x,t) + E_{21}(x+\Delta x, t+\Delta t)\big]\big[E_{11}^*(x,t) + E_{21}(x+\Delta x, t+\Delta t)\big]\Big\rangle \\ &= \langle E_{11}E_{11}^*\rangle + \langle E_{21}E_{21}^*\rangle + 2\mathrm{Re}\Big\langle E_{11}(x,t)\, E_{21}^*(x+\Delta x, t+\Delta t)\Big\rangle, \end{aligned} \tag{3}$$

in which the first two terms describe the energy of the interacting beams E_{11} and E_{21} and the third term is the result of their interference in the form of spatial and temporal correlation function, which can be written for a stationary field in the following form:

$$\Big\langle E_{11}(x,t)\, E_{21}^*(x+\Delta x, t+\Delta t)\Big\rangle = B_{12}(\Delta x, \Delta t). \tag{4}$$

The light transmission through the interferometer is analyzed using the normalized spatial and temporal correlation function

$$\Omega_{12}(\Delta x, \Delta t) = \frac{\big\langle E_{11}(x,t)\, E_{21}(x+\Delta x, t+\Delta t)\big\rangle}{\sqrt{\langle E_{11}^2\rangle\langle E_{21}^2\rangle}}. \tag{5}$$

Having transformed expression (5), we obtain

$$I_{P_1} = I_{11}(P_1) + I_{21}(P_1) + 2\mathrm{Re}\,\Omega_{12}(\Delta x, \Delta t)\sqrt{I_{11}(P_1)\, I_{21}(P_1)}, \tag{6}$$

where $I_{11}(P_1)$ and $I_{21}(P_1)$ are the intensities of the E_{11} and E_{21} beams at the P_1 point (at the first output of interferometer).

Similarly, for the second output of interferometer (point P_2), we have

$$I_{P_2} = I_{22}(P_2) + I_{12}(P_2) + 2\mathrm{Re}\,\Omega_{12}(\Delta x, \Delta t)\sqrt{I_{22}(P_2)\, I_{12}(P_2)}. \tag{7}$$

Based on relations (5)–(7) and the energy conservation law, one can write

$$2\mathrm{Re}\,\Omega_{12}(\Delta x, \Delta t)\sqrt{I_{11}(P_1)\, I_{21}(P_1)} + 2\mathrm{Re}\,\Omega_{12}(\Delta x, \Delta t)\sqrt{I_{22}(P_2)\, I_{12}(P_2)} = 0. \tag{8}$$

Having analyzed expression (8), one can conclude that, when a plane monochromatic wave passes through a passive interferometer, fields with an inverse spatial and temporal intensity distribution are formed at its outputs. When a signal+noise additive mixture arrives at the interferometer input, the result of interaction of these fields is determined by their spatial and temporal coherent properties and the relative spatial and temporal mismatches (Δx, Δy, and Δt) of interferometer arms. Depending on the combination of the aforementioned factors, one can process interferometric signals to solve different problems related to selection of desired signal against the background of additive noise. When the interferometer arms are characterized by zero mismatch ($\Delta x = 0$, $\Delta y = 0$, $\Delta t = 0$), its optical scheme can be described in terms of equivalent plane-parallel plate. An analysis of this equivalent scheme leads to the following important conclusion: there is a potential possibility of concentrating the entire light energy at only one of the interferometer outputs. The situations differing from that described above have some specific features, which are presented in Figs. 1–3. These figures show dependences illustrating the qualitative changes in the normalized spatial and temporal correlation functions of the signal+noise additive mixture, $\Omega_{12}(\Delta x, \Delta t)$ and $\Omega_{21}(\Delta x, \Delta t)$, as well as their components related to the signal ($\Omega_{\mathrm{s}_{12}}(\Delta x, \Delta t)$, $\Omega_{\mathrm{s}_{21}}(\Delta x, \Delta t)$) and noise ($\Omega_{\mathrm{п}_{12}}(\Delta x, \Delta t)$, $\Omega_{\mathrm{п}_{21}}(\Delta x, \Delta t)$) for different situations:

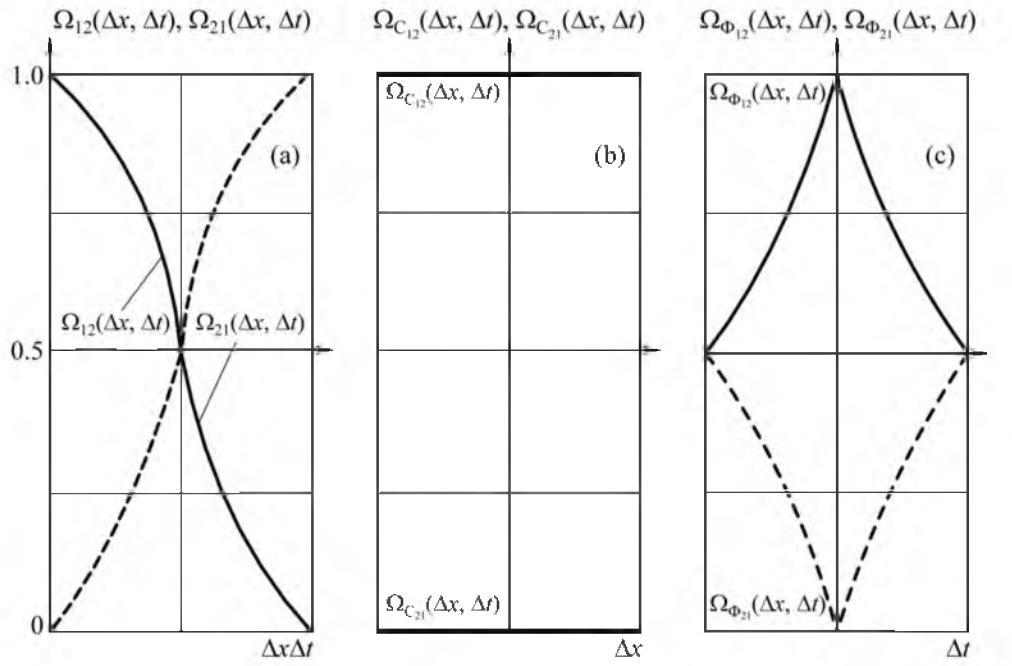

Fig. 1. (a) Normalized spatial and temporal correlation functions of radiation at the interferometer outputs and their components determined by (b) a signal from a point object with low temporal coherence and (c) radiation from uniformly spatially distributed noise with low temporal coherence.

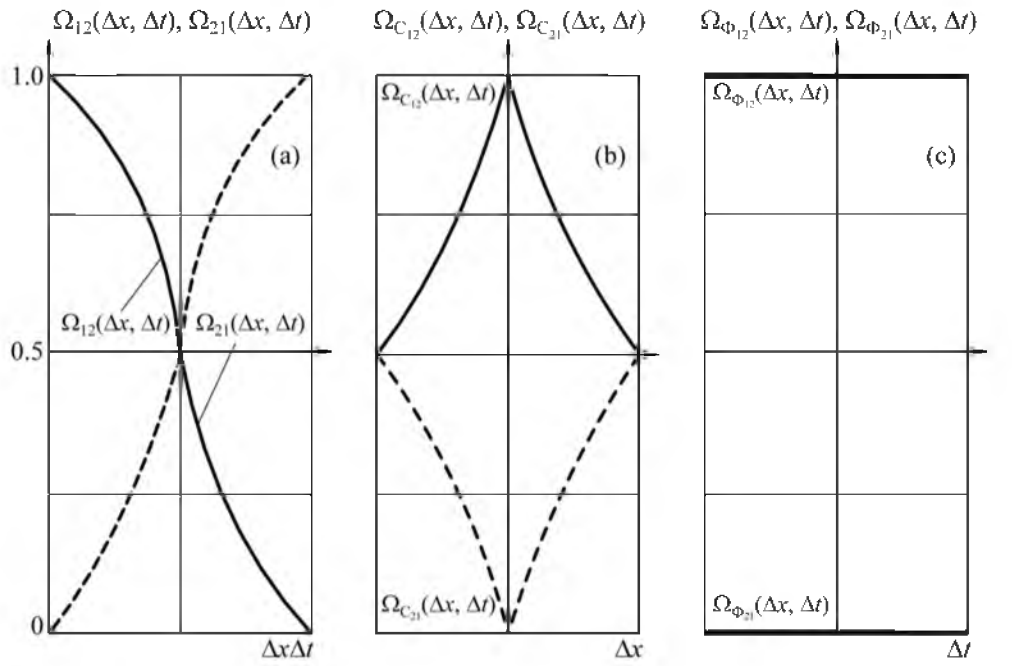

Fig. 2. (a) Normalized spatial and temporal correlation functions of radiation at the interferometer outputs and their components determined by (b) a signal from a point object with low temporal coherence and (c) spatially matched point noise with high temporal coherence.

(i) observation of a signal from a point object with a low temporal coherence against the background of noise with uniform spatial distribution and low temporal coherence (Fig. 1);

(ii) observation of a signal from a point object with a low temporal coherence against the background of point noise (spatially aligned with this object) with high temporal coherence (Fig. 2);

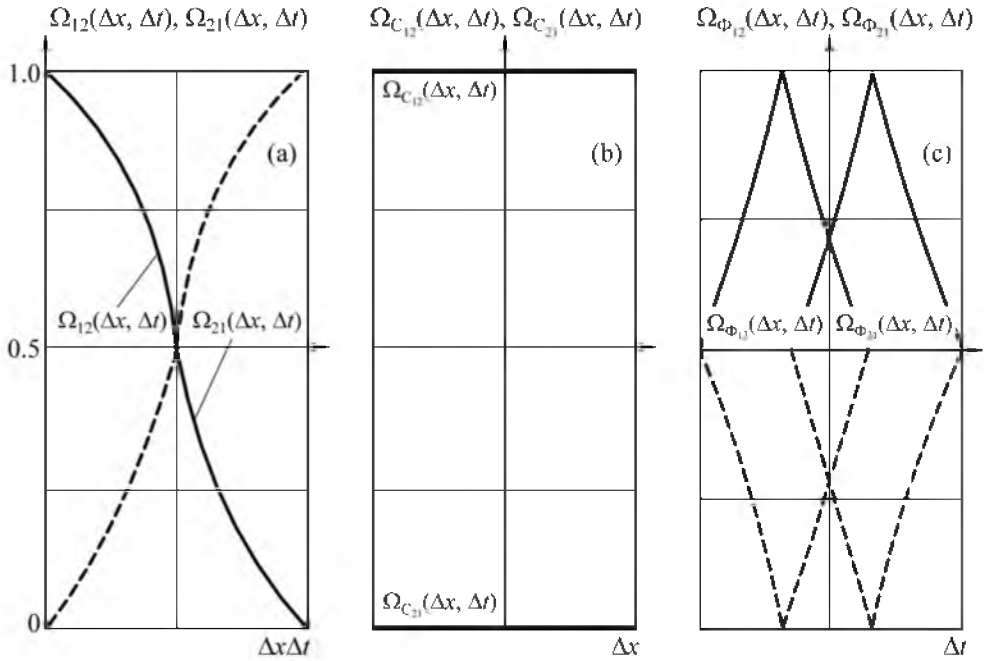

Fig. 3. (a) Normalized spatial and temporal correlation functions of radiation at the interferometer outputs and their components determined by (b) a signal from a point object with low temporal coherence and (c) a signal against the background of spatially mismatched point noise with low temporal coherence.

(iii) observation of signal from a point object with low temporal coherence against the background of spatially mismatched point noise with low temporal coherence (Fig. 3).

An analysis of the dependences presented in Fig. 1 shows the following. When a signal from a point object with low temporal coherence is observed against the background of uniformly spatially distributed noise with low temporal coherence, introduction of spatial mismatch of interfering beams by a value exceeding the spatial coherence length of the background but smaller than the spatial coherence length of the signal, directs the entire energy of useful signal into one of the interferometer arms and distributes the external background energy between the arms. When observing a signal from a point object with low temporal coherence against the background of spatially matched point noise with high temporal coherence (see Fig. 2), the introduction of temporal mismatch of beams by a value exceeding the temporal coherence length of the signal but smaller than the temporal coherence length of the noise makes it possible to direct the noise energy into only one interferometer arm and distribute the signal energy between the arms. An analysis of the dependences shown in Fig. 3 indicates the following. When a signal from a point object with low temporal coherence is observed against the background of spatially mismatched point noise with low temporal coherence, an interference signal of only noise and the non-interfering signal component can be formed at the interferometer output. In this case, the useful signal is proportionally distributed between the interferometer arms. This result is obtained by tuning the interferometer optical axis to the point noise and introducing a spatial mismatch of interfering beams by a value exceeding the spatial coherence length of the signal.

2.2. Experimental Study of Additive-Noise Suppression

The possibility of suppressing noise radiation by interferometric methods was experimentally verified by physical modeling under laboratory conditions. A schematic of the experimental setup is shown in Fig. 4.

In this experiment, we investigated the possibility of selecting radiation from a point signal source against the intense background formed by a point noise source. To this end, a signal and a noise from two independent sources were applied at the interferometer input. The interferometer optical axis was aligned with the direction to the noise source, and an interference pattern of light from this source, with a period determined by the interferometer base, was observed at the interferometer output. The interferometer arms were spatially mismatched by introducing a Dove prism into one of them (to rotate the corresponding beam by 180° [11]) and compensate for the arising interferometer mismatch by inserting an optical delay line (equivalent plane-parallel plate)

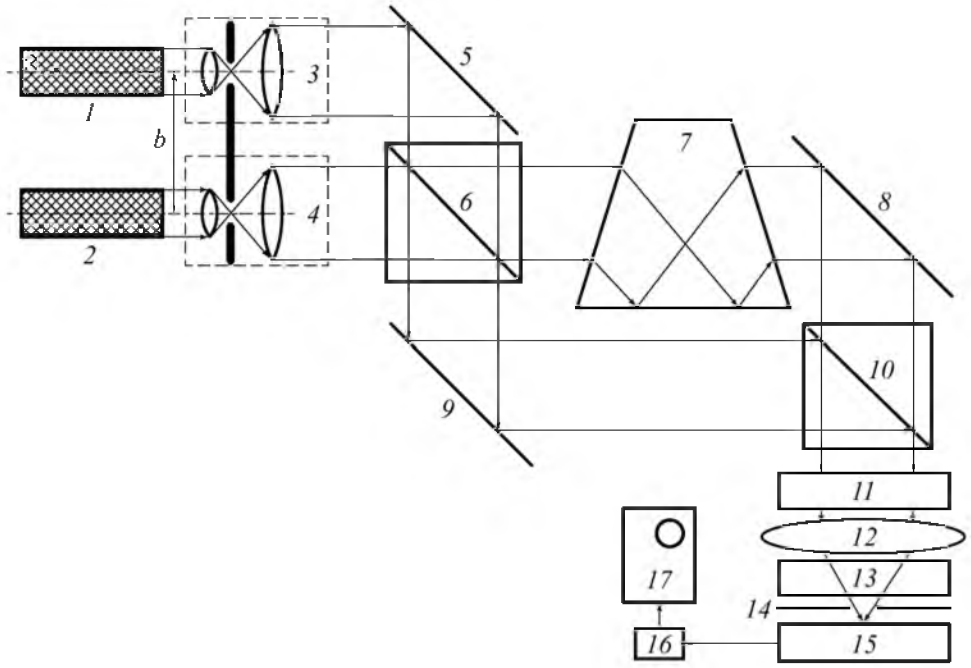

Fig. 4. Block diagram of the experimental setup: lasers (*1*, *2*), condensers (*3*, *4*), mirror (*5*), interferometer elements (*6*–*10*), filter (transparency) (*11*), lens (*12*), rotating plate (*13*), slit (*14*), photoelectron multiplier (*15*), integrator (*16*), and oscilloscope (*17*).

into the other arm. The useful signal was selected by screening the interference pattern from the noise source with a controlled transparency forming absorption regions with a period corresponding to the interference pattern period. The useful signal was also attenuated in this case. The attenuation coefficient of the useful signal is determined by the ratio of the total transmission and absorption areas of the optical transparency within the signal beam.

The results demonstrating the possibilities of suppressing intense point noise and selecting a useful signal as a result of interferometric processing are shown in Fig. 5 in the form of diagrams of photodetector output voltage on oscilloscope screen, which correspond to the spatial distribution of signal and noise intensities in the initial state (Fig. 5(a)) and after passing through the controlled transparency (Fig. 5(b)) [12]. The experiment demonstrated that a signal can be selected against a noise background

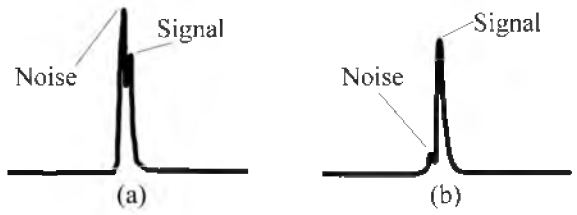

Fig. 5. Results of experimental study: signal and noise at the (a) input and (b) output of interferometric processing device.

when signal and noise sources cannot be resolved according to the Rayleigh criterion and that noise can be significantly suppressed (by one and a half to two orders of magnitude).

3. SUBTRACTION OF ADDITIVE NOISE IN ACTIVE INTERFEROMETER

3.1. Adaptive Filtering of Signals in an Active Interferometer

In contrast to passive optical systems, an active interferometer allows one to use a channel of probe signal formation to process optical signals. Let us consider the specific features of processing (using active interferometric methods) signals scattered by some object. To this end, we will use the classical concept of electromagnetic fields [13], which, in contrast to the quantum-mechanical approach, makes it possible to present descriptively the results obtained. Due to this, one can reveal the procedures that must be performed with optical fields to obtain the desired result.

Let us assume that a distant object is exposed to a probe signal $E_{\text{ps}}(\mathbf{r}, t)$ with a complex spatial structure. Then the distribution of the field $E_{\text{i}}(\mathbf{r}, t)$ in the image plane is a superposition of the field $E_{\text{ps}}(\mathbf{r}, t)$ (signal) scattered by the object and the additive noise $n(\mathbf{r}, t)$:

$$E_{\text{i}}(\mathbf{r}, t) = E_{\text{ps}}(\mathbf{r}, t)\,\sigma(\mathbf{r}) + n(\mathbf{r}, t), \qquad (9)$$

where $\sigma(\mathbf{r})$ is the complex reflectance of the object surface.

For an object exposed to probe signals $E_{ps}(\mathbf{r}, t)$, we have

$$E_i(\mathbf{r}, t_i) = E_{ps}(\mathbf{r}, t_i)\,\sigma(\mathbf{r}) + n(\mathbf{r}, t_i),\ i = 1, 2. \quad (10)$$

Let the interval $\Delta t = t_2 - t_1$ be much narrower than the interval of additive-noise temporal coherence; under these conditions, one can assume the following condition to be satisfied:

$$n(\mathbf{r}, t_1) \approx n(\mathbf{r}, t_2). \quad (11)$$

In this case,

$$E_i(\mathbf{r}, t_1) - E_i(\mathbf{r}, t_2) \cong \left[E_{ps}(\mathbf{r}, t_1) - E_{ps}(\mathbf{r}, t_2)\right]\sigma(\mathbf{r}). \quad (12)$$

According to this relation, when fields with different spatial structures are successively formed in the image plane near the object, there is a potential possibility of implementing one of the ways of spatial filtering, specifically, to subtract additive noise.

Let us analyze the procedure of subtracting received additive noise in an active two-arm interferometer (Fig. 6). Our purpose is to obtain an expression describing the complex amplitude field at the input of photodetector *7*. To this end, we will introduce the following designations: r_{c3} and r_{c4} are the reflectances of beam splitters *2* and *3* for the signals arriving at their first inputs; t_{c3} and t'_{c4} are the transmittances of beam splitters *2* and *3* for the signals arriving at their first and second inputs; $E_{ob}(\mathbf{r})$ is the complex amplitude of the field scattered by the object at the input of beam splitter *2*; $E_n(\mathbf{r})$ is the complex amplitude of additive noise at the input of beam splitter *2*; and $A_1(\mathbf{r})$ and $A_2(\mathbf{r})$ are functions describing the amplitude modulation of the first and second probe pulses, respectively, performed by an array of amplitude modulators.

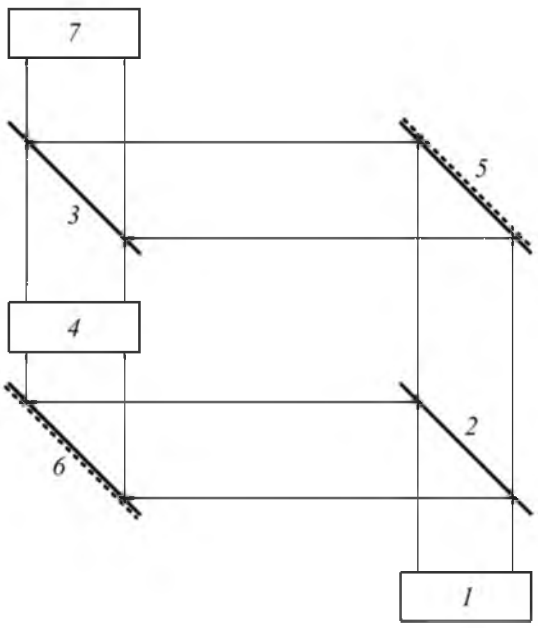

Fig. 6. Block diagram of a two-arm interferometer: laser (*1*), beam splitters (*2*, *3*), delay line (*4*), mirrors (*5*, *6*), and photodetector (*7*).

We also assume that the reflectances of mirrors *5* and *6* are identical and equal to r_3. The optical signal $E_1(\mathbf{r})$, reflected from beam splitter *2* and mirror *6*, delayed in optical delay line *4*, and reflected from beam splitter *3*, can be described by the expression

$$E_1(\mathbf{r}) = \frac{1}{2} r_{c3} r_3 r_{c4}\left[A_1(\mathbf{r})\,E_{ob}(\mathbf{r}) + E_n(\mathbf{r})\right]. \quad (13)$$

The signal $E_2(\mathbf{r})$, transmitted by beam splitter *2*, reflected from mirror *5*, and transmitted through beam splitter *3*, can be written in the form

$$E_2(\mathbf{r}) = \frac{1}{2} r_3 t_{c3} t_{c4}\left[A_2(\mathbf{r})\,E_{ob}(\mathbf{r}) + E_n(\mathbf{r})\right]. \quad (14)$$

The complex amplitude $E_\Sigma(\mathbf{r})$ at the photodetector input is described by the expression

$$\begin{aligned} E_\Sigma(\mathbf{r}) &= E_1(\mathbf{r}) + E_2(\mathbf{r}) \\ &= \frac{1}{2} r_3\left[t_{c3} t_{c4} A_2(\mathbf{r}) + r_{c3} r_{c4} A_1(\mathbf{r})\right] E_{ob}(\mathbf{r}) \\ &\quad + \frac{1}{2} r_3 (t_{c3} t_{c4} + r_{c3} r_{c4}) E_n(\mathbf{r}). \end{aligned} \quad (15)$$

Let us choose the parameters t_{c3}, t_{c4}, r_{c3}, and r_{c4} of beam splitters *2* and *3* so as to satisfy the condition

$$t_{c3} t_{c4} + r_{c3} r_{c4} = 0. \quad (16)$$

In this case, the additive noise is subtracted and expression (15) can be rewritten in the form

$$E_\Sigma(\mathbf{r}) = \frac{1}{2} r_3\left[t_{c3} t_{c4} A_2(\mathbf{r}) + r_{c3} r_{c4} A_1(\mathbf{r})\right] E_{ob}(\mathbf{r}). \quad (17)$$

For example, in the particular case at $t_{c3} = t_{c4} = 1/2$ and $r_{c3} = r_{c4} = (1/2)\exp(j\pi/2)$ ($r_3 \neq \exp(j\pi/2)$), the following relation holds true:

$$E_\Sigma(\mathbf{r}) = \frac{1}{8} r_3\left[A_2(\mathbf{r}) - A_1(\mathbf{r})\right] E_{ob}(\mathbf{r}). \quad (18)$$

According to (18), a signal without additive noise arrives from the interferometer output to the photodetector input. Thus, if the condition $A_2(\mathbf{r}) - A_1(\mathbf{r}) = \text{const} \neq 0$ is satisfied, one can form an object image that is undistorted by additive noise and atmospheric inhomogeneity.

The above-considered operation mode of two-arm interferometer can be applied when there is a possibility of forming a spatial and temporal structure of probe signal in the image plane near the object,

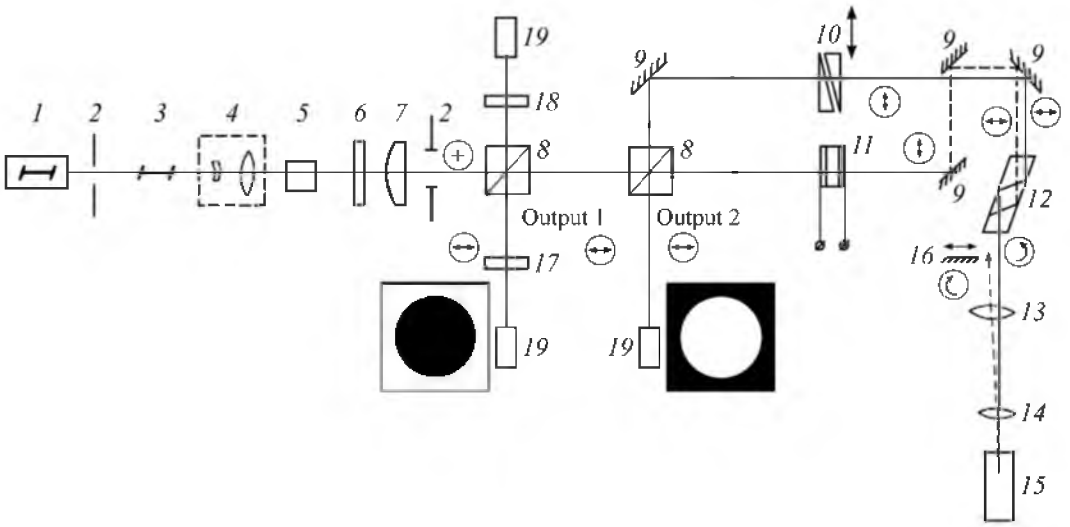

Fig. 7. Block diagram of an experimental breadboard of self-aligning phase-conjugate interferometer: laser (*1*), diaphragm (*2*), laser amplifiers (*3*), collimator (*4*), second-harmonic generator based on KDP crystal (*5*), SZS-21 optical filter (*6*), cylindrical lens, $f = 50$ cm (*7*), beam-splitting cubes (*8*), mirror (*9*), attenuator (*10*), half-wave modulator based on KDP crystal (*11*), Fresnel rhomb (*12*), spherical lens, $f = 100$ cm (*13*), spherical lens, $f = 10$ cm (*14*), cell filled with benzene (*15*), adjusting mirror for checking system in the collimation mode (*16*), polarization analyzer (*17*), neutral light filter (*18*), and photoelectron multiplier FEU-36 (*19*).

which changes from pulse to pulse according to a specified law. Interferometric compensation for additive noise may also occur with an increase in the number of pairs of probe-signal pulses with different spatial and temporal structures. If signals scattered by an object exposed to different pairs of probe pulses with corresponding spatial structures are applied at the input of a two-arm interferometer (see Fig. 6), the signal at the difference output of the interferometer is a composition averaged over realizations.

It is rather difficult to apply the above-described processing methods in practice because of the significant spatial instability of the addition and subtraction regions at the corresponding interferometer outputs, which is due to various destabilizing factors of external and internal origin. These negative factors can be eliminated using interferometers possessing a ray path difference in the interferometer arms and a rather high quality of interferometer elements. An efficient way to eliminate these instabilities is to design self-aligning interferometers equipped with an element responsible for phase matching of extremely weak optical signals. A possibility of using a simulated Brillouin scattering (SBS) mirror as a phase-conjugate element was demonstrated in [14].

3.2. Experimental Study of Additive-Noise Suppression

To carry out experiments on additive-noise suppression in a self-aligning interferometer, we designed an experimental setup, which is schematically shown in Fig. 7. This setup includes a Mach–Zehnder interferometer, a SBS phase-conjugate mirror, and a system of nonreciprocal optical elements. These elements allow one to make the optical path nonreciprocal in the forward and backward directions in one of the interferometer arms. Here, nonreciprocal elements are Fresnel rhomb *12* and half-wave modulator *11* based on a potassium dihydrophosphate (KDP) crystal.

When carrying out the experiment, we verified the fundamental possibility of implementing stable compensation for spatially smooth noise signals with a finite coherence length L_{coh}. The phase shift $\Delta\varphi_1$ in the first interferometer arm was controlled by changing the voltage U across modulator *11* from 0 to U_1. Since a light beam that is matched with the beam propagating in the forward direction propagates in the backward direction in the second interferometer arm, all phase distortions in the second arm are automatically compensated for. In view of this, the light beams with a phase shift $\Delta\varphi_1$ propagating in the backward direction in the interferometer arrive at the beam-splitting surface of element *8*. A phase shift $\Delta\varphi_1$ equal to π was implemented by fitting a certain value of voltage U applied to modulator *11*, as a result of which light fields were subtracted at the second output of the first beam-splitting cube *8* (Fig. 8(a), central part), whereas at the second output of the first cube *8* the fields were added (Fig. 8(b), central part). It was also experimentally demonstrated that the use of an SBS mirror in the interferometer significantly lowers the require-

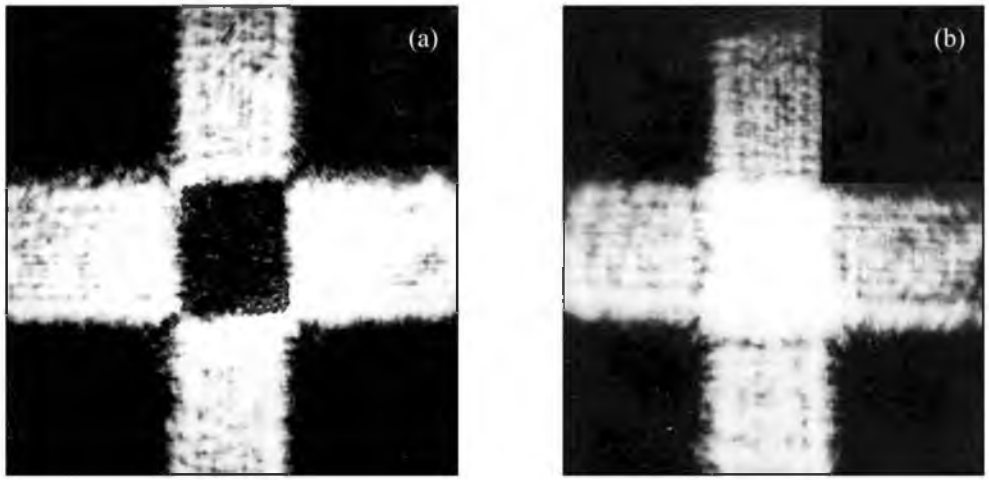

Fig. 8. Results of (a) subtracting and (b) adding signals at the outputs of interferometric processing device.

ments to the ray path difference in the interferometer arms and to the quality of interferometer elements; it also allows one to weaken to a great extent the effect of random malfunctions of the interfering-beam phase (caused by various interfering factors) on the subtraction (addition) result. The degree of noise suppression can be controlled by changing the SBS threshold for the useful signal [14]; this can be done by choosing an acousto-optic medium with a corresponding spontaneous scattering linewidth and using known methods to reduce the SBS threshold (see, for example, [15]).

We also experimentally estimated the effect of external-field amplitude noise on the output characteristics of active interferometer. It was found that, at a variance of input signal amplitude $\sigma_{in}^2 \cong 1.10748 \times 10^{-3} (\mathrm{W\,m^{-2}})^2$ and a mean intensity providing stationary operation of SBS mirror, the variance of the output signal in the difference channel was $\sigma_{out}^2 \cong 1.02769 \times 10^{-3} (\mathrm{W\,m^{-2}})^2$. Based on this finding, we concluded that fluctuations of the output-signal amplitude are basically determined by input-signal fluctuations; this correlation is in good agreement with the results of [16], where a quantum-mechanical approach to active interferometers was developed.

4. CONCLUSIONS

We proposed some interferometric methods for suppressing additive noise in passive and active interferometers. The technical feasibility of these methods was demonstrated and their efficiency was experimentally confirmed. The results obtained can be applied to solve various problems implying the use of interferometric methods, as well as measurement and monitoring tools.

REFERENCES

1. I.V. Skokov, *Multipath Interferometers in Measurement Technique* (Elektronika, Moscow, 1989) [in Russian].
2. V.P. Koronkevich, V.S. Sobolev, and Yu.N. Dubnishchev, *Laser Interferometry* (Nauka, Novosibirsk, 1983) [in Russian].
3. V.S. Sobolev and G.A. Kashcheeva, "Methods of Active Interferometry with Frequency Modulation," Measurement Techniques. **53**(3), 333 (2010).
4. V.S. Sobolev, E.N. Utkin, A.M. Scherbachenko, A.A. Stolpovsky, and G.A. Kashcheeva, "Active Laser Interferometry: Status and Prospects," Optoelectron., Instrum. Data Processing. No. 6, 4 (2004).
5. V.P. Koronkevich, A.G. Poleshuk, A.G. Sedukhin, and G.A. Lenkova, "Laser Interferometric and Diffractive Systems," Comp. Opt. **34**(1), 4 (2010).
6. L.A. Borynyak and Yu.K. Nepochatov, "Holographic Interferometer to Determine the Deformation Displacement Fields in Microelectronics," Technol. Electron. Industry. No. 3, 82 (2007).
7. V.V. Azarova and T.V. Tsvetkova, "Method of Incoherent Interferometry for Monitoring Mirror Quality in Precise Measurement Systems," http://nuclphys.sinp.msu.ru/school/s08/s08_20.pdf
8. V.V. Bukin, S.V. Garnov, A.A. Malyutin, and V.V. Strelkov, "Interferometric Diagnostics of Femtosecond Laser Microplasma in Gases," in *Proceedings of the Prokhorov General Physics Institute*. Vol. 67: *Multicharged Laser Microplasma of Gases*. Ed. by S.V. Garnov (Nauka, Moscow, 2011), pp. 3–31 [in Russian].
9. *Laser Ranging*. Ed. by N.D. Ustinov (Mashinostroenie, Moscow, 1982) [in Russian].
10. V.M. Nikitin, V.N. Fomin, A.I. Nikolaev, and I.L. Borisenkov, *Adaptive Noise Protection in Optoelectronic Information Systems* (Izd-vo BelGU, Belgorod, 2008) [in Russian].

11. V.M. Nikitin, S.G. Garanin, and V.N. Fomin, *Adaptive Noise Protection of Optoelectronic Sensors (for Control and Navigation Systems)* (Izd-vo MGU, Moscow, 2011) [in Russian].
12. V.M. Nikitin, V.N. Fomin, and E.G. Kolomiitsev, *Optoelectronic Astrophysical Observations under Noisy Conditions* (Izd-vo MGU, Moscow, 2012) [in Russian].
13. S.M. Rytov, Yu.A. Kravtsov, and V.I. Tatarskii, *Introduction to Statistical Radiophysics* (Nauka, Moscow, 1978) Pt. 2 [in Russian].
14. V.M. Nikitin, V.N. Fomin, and E.G. Kolomiitsev, *Adaptive Noise Protection in Laser and Optoelectronic Information Systems* (Izd-vo BelGU, Belgorod, 2008) [in Russian].
15. V.R. Belan, A.G. Lazarenko, V.M. Nikitin, and A.V. Polyakov, "Stimulated Brillouin Scattering Mirrors Made of Capillary Waveguides," Sov. J. Quantum Electron. **17**(1), 122 (1987).
16. S.N. Bagayev, A.A. Kurbatov, and E.A. Titov, "Quantum Theory of an Active Interferometer," Quantum Electron. **27**(10), 875 (1997).